



HAL
open science

How Adsorption of Pheromones on Aerosols Controls Their Transport

Ludovic Jami, Thomas Zemb, Jérôme Casas, Jean-François Dufrêche

► **To cite this version:**

Ludovic Jami, Thomas Zemb, Jérôme Casas, Jean-François Dufrêche. How Adsorption of Pheromones on Aerosols Controls Their Transport. ACS Central Science, 2020, 6 (9), pp.1628-1638. 10.1021/acscentsci.0c00892 . hal-02924943

HAL Id: hal-02924943

<https://hal.umontpellier.fr/hal-02924943>

Submitted on 25 May 2021

HAL is a multi-disciplinary open access archive for the deposit and dissemination of scientific research documents, whether they are published or not. The documents may come from teaching and research institutions in France or abroad, or from public or private research centers.

L'archive ouverte pluridisciplinaire **HAL**, est destinée au dépôt et à la diffusion de documents scientifiques de niveau recherche, publiés ou non, émanant des établissements d'enseignement et de recherche français ou étrangers, des laboratoires publics ou privés.

How Adsorption of Pheromones on Aerosols Controls Their Transport

Ludovic Jami, Thomas Zemb, Jérôme Casas, and Jean-François Dufrière*

Cite This: *ACS Cent. Sci.* 2020, 6, 1628–1638

Read Online

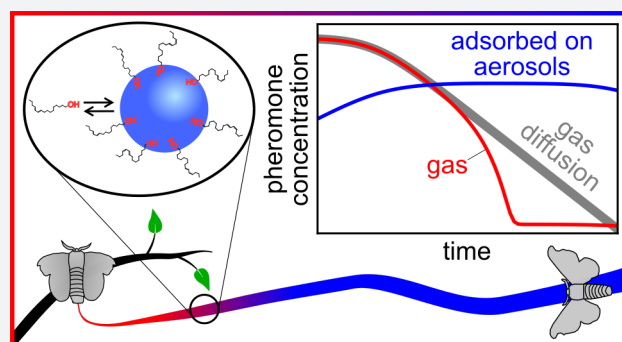
ACCESS |

Metrics & More

Article Recommendations

Supporting Information

ABSTRACT: We propose a general transport theory for pheromone molecules in an atmosphere containing aerosols. Many pheromones are hydrophobic molecules containing polar groups. They are low volatile and have some properties similar to those of hydrotropes. They therefore form a nonsoluble film at the water–air interface of aerosols. The fate of a small pheromone puff in air is computed through reaction-diffusion equations. Partitioning of pheromones between the gas and the aerosol surface over time is studied for various climate conditions (available aerosol surface) and adsorption affinities (energy of adsorption). We show that, for adsorption energy above $30 k_B T$ per molecule, transport of pheromones on aerosols dominates over molecular transport typically 10 s after pheromone emission, even when few adsorbing aerosols are present. This new communication path for airborne chemicals leads to distinctive features including enhanced signal sensibility and increased persistence of pheromone concentration in the air due to slow diffusion of aerosols. Each aerosol droplet has the ability to adsorb thousands of pheromones to the surface, keeping a “history” of the atmospheric content between emission and reception. This new mechanism of pheromone transport leads to dramatic consequences on insect sensing revisiting the way we figure the capture of chemical signals.



INTRODUCTION

Chemical communication through sex pheromones is critical for insect life, enabling mate finding for reproduction. Communication with sex pheromones requires persistence of the olfactory signal in the air to recruit males far from the source. After release, pheromones are thought to be dispersed as gas molecules.^{1–3}

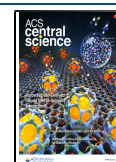
Nevertheless, many pheromones, regarding their chemical structure, are typical low-volatile organic molecule of molar mass 200–400 combining rigidity of some parts, hydrocarbon chains, very apolar sites, polarizability with aromatic rings, as well as polar groups such as OH. Unlike lipids, they have good solubility in apolar solvents. Unlike detergents and surfactant molecules, pheromones are not soluble in water. They are close to neutral hydrotropes that are soluble in water and in solvo-surfactants,^{4–6} except for water solubility. They have therefore a high affinity for the water–air interface, forming an insoluble monolayer film with an area per site of typically less than $1 \text{ nm}^2 \text{ molecule}^{-1}$.

One good example is given by bombykol, from the moth *Bombyx mori* which is a model species for chemical communication.⁷ It is composed of a 16C-long carbon chain and an alcohol headgroup. Its boiling point is predicted to be $298 \text{ }^\circ\text{C}$, and its saturation pressure is 7.5 Pa .⁸ Thus, it is a typically low-volatile compound that can be expected to be found in the aerosol phase. More generally, most known

pheromones used by moths are composed of a carbon chain of 10–18 carbons with a polar headgroup at its end, mostly an alcohol, acetoxy, or formyl group. The major part of the other moth pheromones have a carbon chain and an epoxy group and thus can also be seen to have a polar head and a tail, the latter composed of two carbon chains of different lengths.⁹ Such chemicals are rather likely to stay in a condensed phase or to show aggregating behavior in the air. Pheromones of a moth and a fly species are found as aerosol droplets in the air when released.^{10,11} Emission of pheromones as microdroplets has also been hypothesized for another moth specie by Schall et al.¹² to explain the identical pheromone blend ratio observed in the insect gland and in the air while the vapor pressures of the molecules differ. These references show the necessity of new descriptions of pheromone transport that do not only consider a gas state. On the other hand, the natural presence of aerosols in the air facilitates aggregation of pheromones on their interface.

Received: July 9, 2020

Published: August 12, 2020



Aerosols are mostly observed as water droplets nucleated around either a microcrystal of salt, an organic nanoparticle from plants, a nanoparticle of clay, a particle of man-made volatile organics from combustion, or a mixture of these components.^{13–16} The crucial point is that any aerosol is in equilibrium with the relative humidity (RH) of the atmosphere: the equilibrium radius depends on the relative humidity in a complex way, and it diverges when humidity is above 95%.¹⁵ Therefore, surfactant pheromones can adsorb on this air–water interface and thus form a monolayer.¹⁷ The area of an aerosol of 100 nm typically allows for up to thousands of adsorbed pheromones with an area per molecule of 0.2 nm². In a dry atmosphere, the aerosol droplet shrinks dramatically, but still more than 10 molecules per aerosol can be adsorbed and form a monolayer. By contrast, absorption of pheromones in the bulk water should be negligible because of the poor solubility of the pheromone long carbon tail. Uptake by the aerosol surface of surfactant molecules has already been demonstrated.^{17–19} Moreover, in area in which insects evolved, plant and soil intense activity participates in aerosol generation and maintains a high relative humidity, from 80% to 100% near the ground (<20m).^{20–23} Additionally, many moths call during the night when humidity is the highest thus increasing aerosol water content. These facts are in favor of the hypothesis of pheromone uptake by the aerosols' aqueous surface during their transport. Interactions between aerosols occur however on a significantly greater time scale.^{13,15}

In this paper we aim to evaluate the likelihood and effect of this uptake by making simple physicochemical considerations and by computing the dynamics of the system. We solve analytically the adsorption–desorption kinetics together with the diffusion of a pheromone puff, as it is translated by the wind. We obtain thereby the partitioning of the gas and adsorbed pheromones over time. To account for various pheromone communication contexts, we consider different values for both the available aerosol surface per volume of air and the adsorption energy ruling the equilibrium partitioning as well as the adsorption and the desorption speed, respectively. We identify parameter values for which uptake by aerosols is significant and show how it fundamentally modifies pheromone transport, compared to simple gas diffusion.

■ ADSORPTION OF PHEROMONE ON AEROSOLS

Chemistry of Aqueous Surface Adsorption. Pheromone transport between the source and the receptor is modeled by a dynamical equilibrium between free molecules and adsorbed molecules at the surface of aerosols, as represented in Figure 1. We model the adsorption of pheromone molecules on aerosol aqueous surfaces by a Langmuir isotherm, generally valid for the monolayer adsorption reaction.²⁴ The Langmuir isotherm describes molecules adsorbing at the water surface on individual sites. The latter represent the size of the pheromone and the resulting excluded volume effects. This leads to the saturation of the aerosol surface at high vapor pressure. Gaseous molecules do not interact together. The concentrations at chemical equilibrium are given by the Langmuir mass action law (MAL):

$$\frac{C_a}{(C_{\text{site}} - C_a)C_g} = K^0 \quad (1)$$

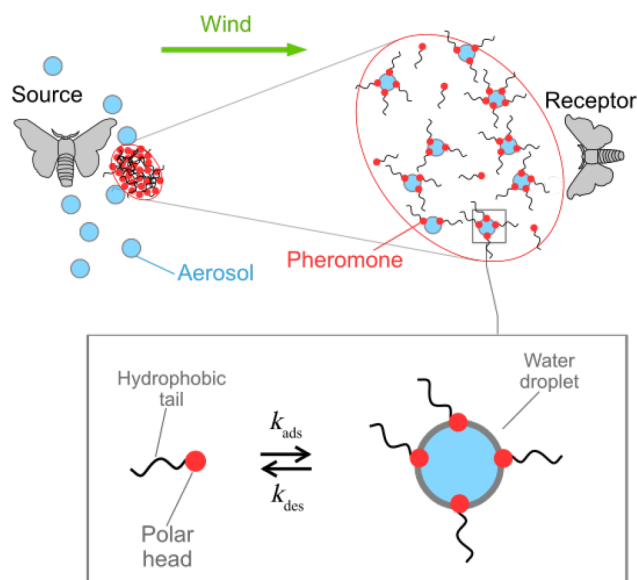


Figure 1. Illustration of the simultaneous advective-diffusive transport and adsorption of pheromones on aerosols.

C_g denotes the number of gaseous pheromones per unit of volume of air, and C_a is the number of adsorbed molecules per unit of volume of air. K^0 is the adsorption equilibrium constant. C_{site} is the number of accessible adsorption sites per unit of volume of air. It is proportional to the aerosol concentration and to their average surface area. C_{site} represents the saturation value of C_a . Far from saturation ($C_a \ll C_s$), at low pheromone concentrations, the chemical equilibrium (eq 1) reads

$$\frac{C_a}{C_g} = K^0 C_{\text{site}} \quad (2)$$

Thus, $K^0 C_{\text{site}}$ is the distribution ratio of pheromones between gas and adsorbed phases.

The equilibrium constant K^0 is linked to the Gibbs energy difference between the gas and the adsorbed phase. Ivanov and collaborators^{24,25} developed a description for surfactant molecules composed of a carbon chain and a nonionic polar headgroup, thus similar to the pheromones that we describe. Generalizing this approach for nonsoluble molecules at a water–air interface (see Appendix A), we obtain the following:

$$K^0 = S_{\text{site}} \delta e^{E_{\text{ads}}/k_B T} \quad (3)$$

E_{ads} is the adsorption energy (which is considered to be positive if adsorption is favorable). k_B is the Boltzmann constant, and T is the temperature (chosen to be 25 °C in our study). S_{site} is the surface of an adsorption site supposed to be closed to the polar headgroup area in a close packed structure (which is typically 16.5 Å²). $\delta = l_{\text{CH}_2} \frac{k_B T}{2\Delta\mu_{\text{CH}_2}}$ is the Ivanov length²⁵ taking into account the rotational constraints at the interface (entropic loss) and the partial solvation of the carbon chain of the molecule as it is oscillating at the water surface. $l_{\text{CH}_2} = 1.26$ Å is the length of a CH₂ group, and $\Delta\mu_{\text{CH}_2} = 1.04 k_B T$ is its free energy of hydration. The adsorption energy reads $E_{\text{ads}} = E_{\text{head}} + \gamma S_{\text{site}}$, where E_{head} is the bounding energy of the hydrophilic headgroup with the water molecules, and γ is the surface tension of water taking into account the disappearance of interfacial area. The main contribution to E_{head} is the H-bonds created between the headgroup and water, which can be

roughly estimated at around $8 k_B T$ per H-bond.²⁶ This model gives a rough estimate of $10 k_B T$ for the adsorption energy of alcohol pheromones (like bombykol) on water. Adsorption energy should be higher for fatty acid pheromones as more H-bonds are involved.

Alternatively,²⁷ considering volatile molecules emitted by plants, Liyana-Arachchi et al. computed the free energy profile between adsorbed and gas states from atomistic simulations by displacing the molecules in the direction orthogonal to the water–air interface. They considered an alcohol molecule, cis-3-hexen-1-ol, which is also composed of a carbon chain and a polar headgroup but with a shorter carbon chain than the pheromones we describe. The free energy profile they obtained has a minima at the water–air interface. This free energy minimum at the interface can be fitted by a harmonic law. The resulting adsorption constant is $K^0 = 1 \times 10^{-16} \text{ cm}^3$, corresponding to an adsorption energy of $E_{\text{ads}} = 16.2 k_B T$.

These different estimates show that adsorption energy of pheromones on aerosols aqueous surface is typically of the order of few $10 k_B T$. Nevertheless we expect the adsorption energy to vary a lot depending on the nature of the pheromone and the composition of aerosols. Additional effects beyond the ones described here can also significantly increase adsorption: mutual attraction of adsorbed pheromone carbon chains or with other adsorbed organics or interaction with dissolved ions. To account for the variety of systems that can be found in the environment we leave the adsorption energy as a parameter to vary in our model, in the range $5\text{--}50 k_B T$, in order to study its influence on pheromone transport. Note that the case of aerosols mostly composed of organics rather than water is also implicitly considered by our description and parametrization of the adsorption constant K^0 as long as the pheromones do not penetrate into the bulk of the organic aerosols.

Kinetics of Surface Adsorption. Kinetics of the adsorption reaction is governed by adsorption and desorption processes, as represented in the box in Figure 1. These processes are supposed to be elementary. This means that gas pheromone molecules (of concentration C_g) adsorb relatively to the rate of encounters with free sites (of concentration $C_s - C_a$). Additionally adsorbed pheromones desorb proportionally to their concentration C_a . Then, the chemical dynamics of gas and adsorbed pheromones reads

$$\frac{dC_g}{dt} = -k_{\text{ads}}(C_{\text{site}} - C_a)C_g + k_{\text{des}}C_a \quad (4)$$

$$\frac{dC_a}{dt} = k_{\text{ads}}(C_{\text{site}} - C_a)C_g - k_{\text{des}}C_a \quad (5)$$

where k_{ads} and k_{des} are the kinetic constants of adsorption and desorption, respectively. Supposing that the adsorption rate corresponds to the collision rate between the free pheromones and the aerosol surface, we obtain from kinetic theory (Hertz relation)

$$k_{\text{ads}} = k_{\text{Hertz}} = \sqrt{\frac{RT}{2\pi M}} S_{\text{site}} \quad (6)$$

R is the perfect gas constant, and M is the molar mass of the pheromone. As a reference we chose $M = 238 \text{ g mol}^{-1}$, the molar mass of bombykol. This relation supposes (i) that pheromone molecules follow the Maxwell–Boltzmann distribution, (ii) that impacts of individual molecules are independent (Poisson processes), and (iii) that every molecule

impacting the surface gets adsorbed. Hypotheses i and ii are true for ideal gas. The third hypothesis is more questionable. Some authors^{28–31} consider a Knudsen correction factor that accounts for the possibility of bouncing back. On the other hand, several molecular dynamic simulations, regarding liquid/vapor systems developed by different groups,^{32–35} support the Hertz relation and the absence of this phenomenon. The Hertz equation corresponds to the transition state theory (TST) approximation³⁶ when the transition state is defined as the surface of the aerosols. In fact, gas pheromones become adsorbed on the aerosol surface. Their concentration in air close to the surface is depleted, and diffusion has to compensate this depletion. Thus, gas diffusion of pheromones toward aerosols can limit the adsorption kinetics depending on the size of the aerosols. This limitation of the adsorption kinetics can be taken into account by modifying the adsorption rate (eq 6) by a factor ϵ that explicitly depends on aerosol radius:³⁷

$$k_{\text{ads}} = \epsilon \sqrt{\frac{RT}{2\pi M}} S_{\text{site}} \quad (7)$$

With $\frac{1}{\epsilon} = 1 + \left(1 - \frac{C_a}{C_{\text{site}}}\right) \frac{0.75 + 0.28Kn}{Kn(1 + Kn)}$ where Kn is the Knudsen number, i.e., the ratio between the mean free path of the pheromone molecule ($\lambda = 0.2 \mu\text{m}$) and the aerosol radius: $Kn = \frac{\lambda}{R_{\text{aero}}}$.

The equilibrium condition imposes the following:

$$\frac{k_{\text{ads}}}{k_{\text{des}}} = K^0 \Leftrightarrow k_{\text{des}} = k_{\text{ads}} K^{0-1} = \frac{k_{\text{ads}}}{\delta S_{\text{site}}} e^{-E_{\text{ads}}/k_B T} \quad (8)$$

This equation illustrates the fact that adsorption and desorption of molecules on a surface are nonactivated processes in agreement with molecular dynamics simulations.^{27,32–35} Finally, within this model, the adsorption kinetics constant k_{ads} is only governed by the Maxwell–Boltzmann distribution in the gas phase. Adsorption kinetics also depends on the concentration of available sites $C_{\text{site}} - C_a$ since the adsorption flux in eqs 4 and 5 is proportional to this quantity. The desorption kinetic constant k_{des} is governed by the adsorption energy E_{ads} (which gives K^0). Indeed, E_{ads} represents the kinetic energy the molecule will have to desorb.

Now let us suppose that no saturation occurs ($C_{\text{site}} \gg C_a$) so that $\epsilon \approx \frac{1}{1 + \frac{0.75 + 0.28Kn}{Kn(1 + Kn)}}$. Figure 2 shows how the adsorption and

desorption times as well as the ϵ factor depend on the aerosol radius. For small aerosol radii, $\epsilon \approx 1$, and thus, its effects on the adsorption kinetic can be disregarded. In the following we consider the assumption $\epsilon = 1$ (Hertz formula) being rigorously valid for small aerosols. With this approximation, arbitrary aerosol size distributions can be conveniently described, due to the sole influence of C_{site} , the total number of sites. See Supporting Information, section A, for further evaluation of the effect of the ϵ factor.

Equations 4 and 5, when no saturation occurs, reduce to

$$\frac{\partial C_g}{\partial t} - k_{\text{ads}}(C_{\text{site}} + K^{0-1})C_g + k_{\text{ads}}C_T = 0 \quad (9)$$

where the total concentration $C_T = C_g + C_a$ is a constant. A characteristic time scale for the adsorption reaction can be extracted from eq 9:

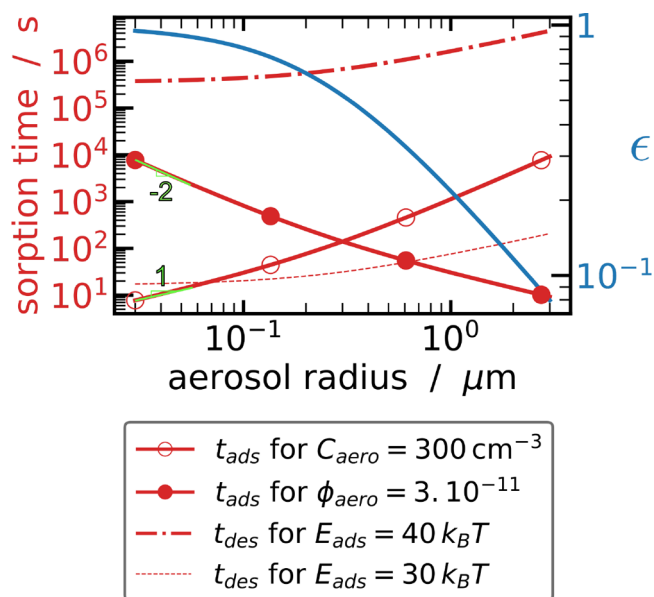


Figure 2. Adsorption and desorption times (red) as functions of the aerosol size. The adsorption time is plotted for two cases, at fixed aerosol concentration (C_{aero}) and at fixed volume fraction (ϕ_{aero}). The desorption time is plotted for two adsorption energies (E_{ads}). On the right axis the ϵ factor, quantifying the limitation of adsorption kinetics due to pheromone diffusion toward aerosols, is also plotted in blue. In the model described below we consider the limit of small aerosol radius, $\epsilon = 1$. In that case, the desorption time is constant, and the adsorption time follows a limiting law (slope -2 and 1 in the thin green solid line); see the Supporting Information, section A, for details.

$$t_{\chi} = \frac{1}{k_{ads}(C_{site} + K^{0-1})} = \frac{K^0}{k_{ads}(C_{site}K^0 + 1)} \quad (10)$$

This characteristic time is shorter than the characteristic time for the adsorption alone $t_{ads} = \frac{1}{k_{ads}C_{site}} = \sqrt{\frac{2\pi M}{RT}} \frac{1}{C_{site}S_{site}} = \sqrt{\frac{2\pi M}{RT}} \frac{1}{4\pi R_{aero}^2 C_{aero}}$. Thus, considering a typical aerosol radius $R_{aero} = 0.3 \mu\text{m}$, the adsorption time t_{ads} and consequently t_{χ} are less than 100 s if the aerosol concentration C_{aero} is more than 220 aerosols per cm^3 of air, within the range of observed values.^{13–15,18,21}

This simple calculation shows that pheromone adsorption is a fast phenomenon compared to the time scale of insect communication (10 min to several hours^{1,12,38,39}) as long as pheromone adsorption is thermodynamically possible. Thus, on this condition insect pheromones are spontaneously adsorbed on atmospheric aerosols, allowing a new communication channel between insects. In that case, information is not transmitted by gas molecules but by aerosols. This is the main point of this Article. The following transport model quantifies the transport by aerosols with respect to gas diffusion.

MODELING PHEROMONE AEROSOL INTERACTION AND THEIR TRANSPORT

Diffusion-Reaction Model. We consider now that the kinetic eqs 4 and 5 hold locally, but we also consider the global transport of pheromones due to gas diffusion, aerosol diffusion, and advection by the wind.⁴⁰

We consider a spherical puff of pheromone with a given initial size, released by a female and transported horizontally by

a laminar wind. The model is described in Figure 1. Mixing of the puff by air turbulence is disregarded in this paper considering that turbulence does not modify adsorption kinetics. In addition, diffusion is the determinant transport mechanism to consider in order to evaluate the aerosol transport of pheromones, prior to turbulent mixing considerations. Indeed diffusion transport is dominant initially when the adsorption reaction is established as we consider puffs smaller than the centimeter scale.^{2,3}

Pheromone transport is described by

$$\frac{\partial C_g}{\partial t} + \mathbf{v} \cdot \nabla C_g = D_g \Delta C_g + k_{abs}(-(C_{site} - C_a)C_g + K^{0-1}C_a) \quad (11)$$

$$\frac{\partial C_a}{\partial t} + \mathbf{v} \cdot \nabla C_a = D_a \Delta C_a - k_{abs}(-(C_{site} - C_a)C_g + K^{0-1}C_a) \quad (12)$$

$\Delta = \frac{1}{r^2} \frac{\partial}{\partial r} \left(r^2 \frac{\partial f}{\partial r} \right)$ denotes the spherical Laplacian operator, and r is the radial position in the puff. $D_g = 10^{-5} \text{m}^2 \text{s}^{-1}$ is the diffusion coefficient of the gas pheromone in the air. The adsorbed pheromones, as they are bounded to the aerosol surface, diffuse in the air in the same way as the aerosol carrying them. Thus, the diffusion coefficient of adsorbed pheromones is equal to the one of aerosols: $D_a = 10^{-10} \text{m}^2 \text{s}^{-1}$.¹⁵ The latter diffusion coefficient is considered constant, and its variations with the radius of the aerosol are not significant because aerosol diffusivity is much slower than gas diffusivity which is the most important feature here (see the Supporting Information, section B). This value of D_a is a representative order of magnitude for the diffusion coefficient of aerosols. \mathbf{v} is the wind speed. By doing a Galilean change of referential and describing the puff in the referential associated with its center of mass, the above equations reduce to

$$\frac{\partial C_g}{\partial t} = D_g \Delta C_g + k_{abs}(-(C_{site} - C_a)C_g + K^{0-1}C_a) \quad (13)$$

$$\frac{\partial C_a}{\partial t} = D_a \Delta C_a - k_{abs}(-(C_{site} - C_a)C_g + K^{0-1}C_a) \quad (14)$$

For a puff of gas pheromone released by the insect, eqs 13 and 14 indicate that pheromone will diffuse as gas for some of them and be adsorbed on aerosols for the others. After a certain chemical time, the adsorbed and gas pheromone will reach an equilibrium distribution ratio, and diffusion of the total pheromone concentration C_T will be a combination of the gas and aerosol diffusion with respect to pheromone partitioning.

Linearization. Equations 13 and 14 are nonlinear with respect to the initial pheromone concentration of the puff, due to the possible saturation of the aerosols. Estimating puff initial pheromone concentration (C_T^i) is a challenging task as a large range of values for pheromone concentrations are given in the literature. From measurements of pheromone release flux of calling a female moth within its immediate surrounding,^{12,39} we estimated C_T^i to be around $5 \times 10^{11} \text{cm}^{-3}$. This value can be considered as an upper bound regarding to the measurement method. An initial concentration of several orders of magnitude lower can be expected in the case of a higher air velocity around the emitting insect.

On the other hand, the maximal adsorption concentration C_{site} is left as a parameter to vary in our model in order to study

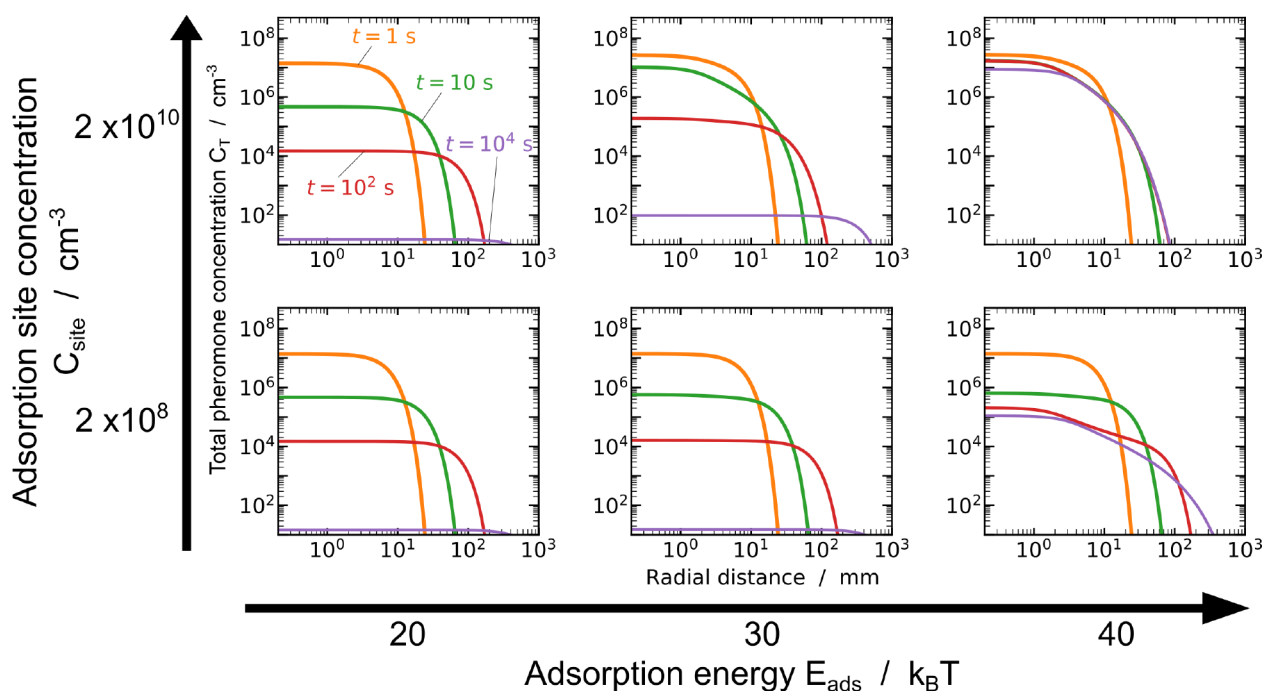


Figure 3. Profiles of total pheromone concentration over time. For high C_{site} and E_{ads} , pheromones are quickly and numerous adsorbed. Therefore, the puff diffuses way less through gas diffusion and stays concentrated and confined in a small volume thanks to aerosols. For small C_{site} and E_{ads} , adsorption on aerosols is low and does not influence the transport of pheromones. Initial puff concentration is $C_T^i = 5 \times 10^9 \text{ cm}^{-3}$, and initial puff radius is $R_i = 1 \text{ mm}$. Log scaled axis.

the influence of changes in aerosol size or concentration on pheromone transport. Environmental data report a large range of values^{13–15,18,21} for these parameters; therefore, C_{site} is expected to vary over several orders of magnitude. Values of C_{site} considered here lie between 6.2×10^7 and $6.2 \times 10^{10} \text{ cm}^{-3}$, which correspond in the case of aerosols of $0.3 \mu\text{m}$ to a concentration of $10\text{--}10^4$ aerosols per cm^3 . For these values of C_{site} , adsorption time (t_{ads}) varies between 2.2 s and 2.2×10^3 s.

Even though highest estimates of C_T^i are way greater than the smallest value accounted for C_{site} , no significant saturation effects should take place for these parameter values. Indeed, gas diffusion always disperses pheromones in the air to concentrations where no saturation can occur. Moreover, a small value of adsorption C_{site} leads to long adsorption time. Consequently, during this time, pheromone molecules diffuse away from loaded aerosols, and they do not saturate it.

Neglecting saturation effects in eqs 13 and 14 yields the following linear system of equations for the evolution of the puff:

$$\frac{\partial C_g}{\partial t} = D_g \Delta C_g - k_{\text{abs}} C_{\text{site}} C_g + k_{\text{abs}} K^{0-1} C_a \quad (15)$$

$$\frac{\partial C_a}{\partial t} = D_a \Delta C_a + k_{\text{abs}} C_{\text{site}} C_g - k_{\text{abs}} K^{0-1} C_a \quad (16)$$

Such a system of linear equations can be solved analytically.

■ SOLUTION AND PARAMETRIC ANALYSIS OF THE TRANSPORT MODEL

Solution of Diffusion-Reaction Equations. Reaction-diffusion eqs 15 and 16 can be solved through normal modes analysis.^{41,42} Applying the spacial Fourier transform yields

$$\frac{\partial \hat{C}_g}{\partial t} = (-D_g q^2 - k_{\text{abs}} C_{\text{site}}) \hat{C}_g + k_{\text{abs}} K^{0-1} \hat{C}_a \quad (17)$$

$$\frac{\partial \hat{C}_a}{\partial t} = k_{\text{abs}} C_{\text{site}} \hat{C}_g + (-D_a q^2 - k_{\text{abs}} K^{0-1}) \hat{C}_a \quad (18)$$

where hat notation (^) denotes here Fourier transforms, and q is the Fourier variable. This system of equations has the form

$$\frac{\partial}{\partial t} \begin{pmatrix} \hat{C}_g \\ \hat{C}_a \end{pmatrix} = M \begin{pmatrix} \hat{C}_g \\ \hat{C}_a \end{pmatrix}, \quad \text{with } M \text{ a matrix. Therefore, we have the}$$

following solution:

$$\begin{pmatrix} \hat{C}_g \\ \hat{C}_a \end{pmatrix} = \exp(Mt) \begin{pmatrix} \hat{C}_{g0} \\ \hat{C}_{a0} \end{pmatrix} \quad (19)$$

where C_{g0} and C_{a0} are the concentrations of gas and adsorbed pheromones at $t = 0$. Eigenvalues of M correspond to the normal modes of the system. Diagonalization of M leads to

$$\exp(Mt) = \frac{s_- e^{s_- t} - s_+ e^{s_+ t}}{s_- - s_+} \mathbf{I} + \frac{e^{s_- t} - e^{s_+ t}}{s_- - s_+} \begin{pmatrix} D_g q^2 + k_{\text{abs}} K^{0-1} & k_{\text{abs}} K^{0-1} \\ k_{\text{abs}} C_{\text{site}} & D_a q^2 + k_{\text{abs}} C_{\text{site}} \end{pmatrix} \quad (20)$$

\mathbf{I} is the 2×2 identity matrix. s_- and s_+ are the eigenvalues of M :

$$s_{\pm} = -\frac{1}{2} (D_g q^2 + D_a q^2 + k_{\text{abs}} C_{\text{site}} + k_{\text{abs}} K^{0-1}) \pm \frac{1}{2} \sqrt{\Delta_q} \quad (21)$$

with

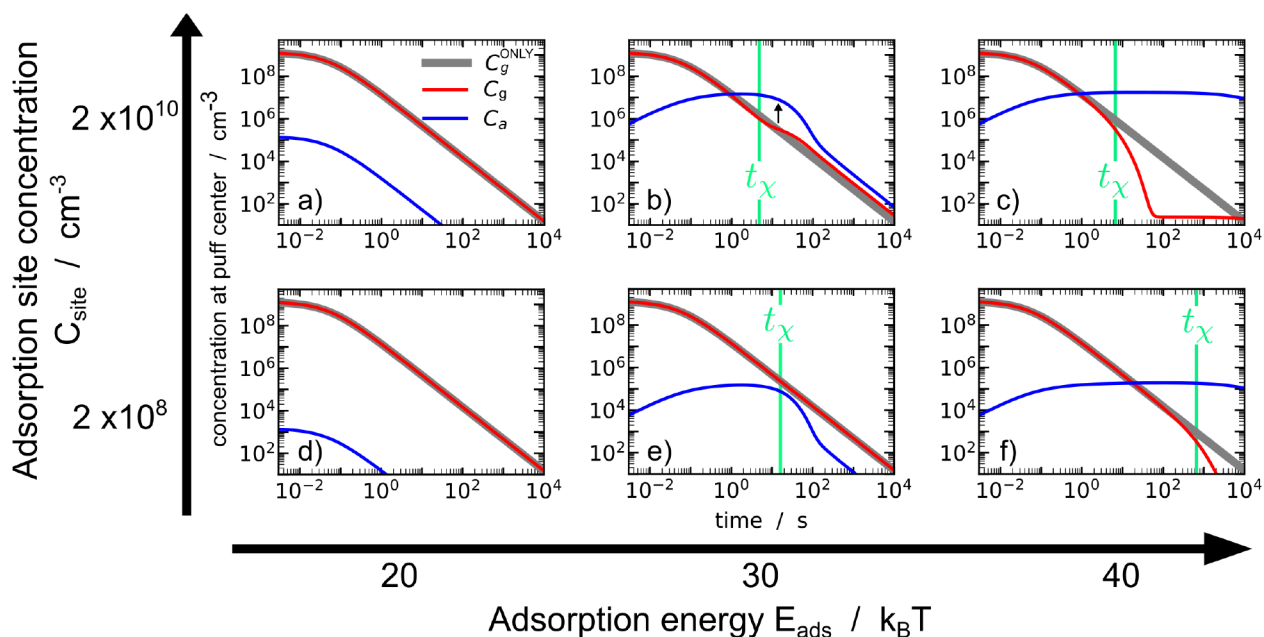


Figure 4. Concentration of pheromones at the center of the puff over time. These graphs illustrate that, after 10^2 s, in most realistic cases, the majority of the tiny amount of emitted pheromones are adsorbed and transported as finite ensembles by individual aerosols. C_g and C_a are, respectively, the concentration of gas and adsorbed pheromones. C_g^{ONLY} is pheromone concentration when no aerosols are present, pheromones remaining in the gas phase. t_χ is the time of the adsorption/desorption reaction (eq 10). When adsorption is favorable (high E_{ads} and C_{site}), adsorbed pheromones become predominant after some time. This slows down the decrease of concentrations due to diffusion. When adsorption is not favorable, only a small proportion of pheromones become adsorbed, and it does not modify the decrease of the concentration. Log scaled axis.

$$\Delta_q = (D_g - D_a)^2 q^4 + 2k_{\text{ads}}(K^{0-1} - C_{\text{site}})(D_a - D_g)q^2 + k_{\text{ads}}^2(C_{\text{site}} + K^{0-1})^2 \quad (22)$$

Equations 20–22 correspond to the Green function, in the Fourier space, of the reaction-diffusion eqs 15 and 16. We thus have an analytic solution of the problem that can be readily computed for a given set of parameters. Two limiting regimes can be obtained:

(1) At large distances, for a puff with a large characteristic size $1/q \gg \sqrt{D_{\text{eff}}t_\chi}$, we have $s_+ \approx -D_{\text{eff}}q^2$ and $s_- \approx -1/t_\chi$. D_{eff} is an effective diffusivity:

$$D_{\text{eff}} = D_g \frac{1}{C_{\text{site}}K^0 + 1} + D_a \frac{C_{\text{site}}K^0}{C_{\text{site}}K^0 + 1} \quad (23)$$

It corresponds to a linear combination of gas and aerosol diffusion, whose weights are the proportion of pheromone in gas and adsorbed phase at chemical equilibrium. s_+ is the diffusion mode, and s_- is the chemical mode that describes the relaxation toward chemical equilibrium as predicted by MAL.

(2) At short distances, for a puff with small characteristic size $1/q \ll \sqrt{D_{\text{eff}}t_\chi}$, $s_+ \approx -D_a q^2$ and $s_- \approx -D_g q^2$. Thus, s_+ and s_- are uncoupled diffusion modes of gas and adsorbed pheromones.

Thus, a puff initially small has the dynamic of two puffs, one made of adsorbed and one made of gas pheromones puffs, diffusing independently. The puff behaves thusly for a time comparable to t_χ . By then, the puff size is larger, and pheromones diffuse with diffusivity D_{eff} ; pheromone partitioning respects MAL locally.

The analytical solution of the model presented here can be used to describe various situations encountered in insect pheromonal communication contexts by simply choosing the

correct parameter values adapted to the considered insect and the local aerosol conditions occurring during insect calling. We further solve the model for various parameter values to present the different regimes that can be encountered.

Parametric Analysis. We consider an initial 1 mm sized Gaussian puff of pheromones only in the gas phase with initial concentration $C_T^i = 5 \times 10^9 \text{ cm}^{-3}$:

$$C_g = \frac{4/3\pi C_T^i}{\sqrt{2\pi}^3} e^{-r^2/2R_i^2} \text{ and } C_a = 0 \quad (24)$$

The puff contains $N_T = \frac{4}{3}\pi R_i^3 C_T^i = 2.110^7$ molecules. Concentration profiles were discretized with a spacial step $\Delta r = 1/30$ mm, and the maximal radius we considered is $N\Delta r = 402493 \times \frac{10^{-3}}{30} \approx 13.4$ m. The spacial step and maximal radius were chosen, respectively, small and high enough to prevent any aliasing effects. Note that as we deal with linear equations here (eqs 15 and 16), concentration scales presented in our figures are simply proportional to the chosen initial concentration value C_T^i . Another C_T^i would not change anything but the concentration scales.

Figure 3 illustrates the concentration profiles obtained for total (gas + adsorbed) pheromone concentration. As time goes, profiles spread more and more on the r -axis, and concentration decreases due to diffusion. However, as we increase site concentration (C_{site}) and adsorption energy (E_{ads}), diffusion is less and less efficient, mainly due to a smaller effective diffusivity (eq 23). This illustrates that a favorable adsorption of pheromones on aerosols implies a reduction of the diffusion of pheromones in the air, so that the puff stays concentrated and keeps a small size during its transport. At high adsorption energy and high concentration of the aerosol surface, the pheromone remains in a centimetric domain after

several hours, whereas gas diffusion would have widespread the molecules in a 1 m large domain. Aerosols keep the number of pheromones per volume of air at a high level over a long time and long distance of transport.

Figure 4 presents concentrations of adsorbed and gas pheromones at the center of the puff as functions of time. The relative importance of adsorption over the desorption process explains the various observed behaviors. For an adsorption energy (E_{ads}) of $40 k_{\text{B}}T$ (Figure 4c,f), the desorption is quasinegligible, and C_{a} increases due to the adsorption process at the same time as C_{g} decreases due to diffusion. The concentration of adsorbed pheromone (C_{a}) becomes higher than the concentration of gas pheromone (C_{g}) after some time. Then, pheromone concentration stops decreasing because they are mainly adsorbed on aerosols, which exhibit a slow diffusion.

For $E_{\text{ads}} = 30 k_{\text{B}}T$ and $C_{\text{site}} = 2 \times 10^{10} \text{ cm}^{-3}$ (Figure 4b), the decreasing of pheromone concentrations is only delayed compared to a case where no aerosols would be present. This is due to two effects. First, the effective diffusivity (eq 23) is smaller than gas diffusion and takes place when the chemical equilibrium is reached. Second (see black arrow in the graph), as the center of the puff becomes depleted of gaseous pheromones, adsorbed pheromones need to be desorbed for diffusion to continue. In other words, at a certain time (~ 3 s), aerosols become excessively loaded in pheromones compared to the amount of gaseous pheromones around them so that desorption is limiting the dilution of pheromones. This effect leads here to a 10-fold increase in pheromone concentration at the center of the puff after few t_{χ} .

For $E_{\text{ads}} = 20 k_{\text{B}}T$ (Figure 4a,d) and for $E_{\text{ads}} = 30 k_{\text{B}}T$ and $C_{\text{site}} = 2 \times 10^8 \text{ cm}^{-3}$ (Figure 4e), desorption is mostly dominant over adsorption, and no delay of the diffusion is observed as pheromones are mostly in the gas phase. For $E_{\text{ads}} = 30 k_{\text{B}}T$ and $C_{\text{site}} = 2 \times 10^8 \text{ cm}^{-3}$, a switch from the adsorbing to desorbing regime is also observable. For $E_{\text{ads}} = 20 k_{\text{B}}T$, chemical processes occur before gas diffusion takes place with very few molecules adsorbed, and equilibrium is instantaneously adapted as diffusion occurs.

To finely describe the transition in parameter values for which pheromone adsorption on aerosols becomes significant, we plotted in Figure 5a,b the concentrations of gas and adsorbed pheromones at the center of a puff 100 s after its emission, as functions of E_{ads} and C_{site} . Drastically different behaviors can be observed whether adsorption energy is above or below $30 k_{\text{B}}T$. Above this threshold, a significant amount of pheromones are adsorbed on aerosols, and C_{a} only varies with adsorption site concentration (because it governs the adsorption process). The number of pheromones per aerosol $N_{\text{a}} = \frac{C_{\text{a}}}{C_{\text{aero}}}$ is also plotted in Figure 5c. It only slightly depends on the aerosol concentration (C_{aero}). Indeed, physically, this quantity does not directly depend on the aerosol concentration. This is due to the fact that a single aerosol equilibrates its number of adsorbed pheromones with the gas ones independently of how many aerosol neighbors it has. The only indirect dependence comes from the dynamics of the gas pheromone concentration (C_{g}) as can be shown by rewriting eqs 15 and 16 in terms of the number of pheromones per aerosols (N_{a}). At short times ($t < t_{\chi}$), C_{g} mainly exhibits a diffusion process which does not depend on C_{aero} (Figure 4). Thus, N_{a} does not depend on this quantity. At long times ($t > t_{\chi}$) once the adsorption is made, the adsorption flux becomes

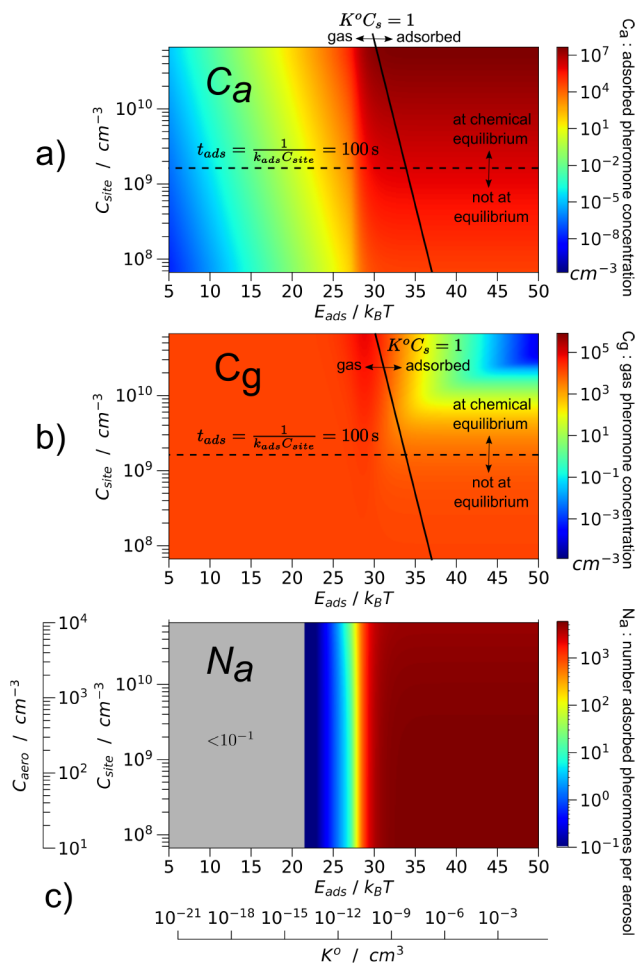


Figure 5. Adsorbed pheromone concentration (C_{a}), gas pheromone concentration (C_{g}), and number of adsorbed pheromones per aerosol (N_{a}) at the center of the puff 100 s after its emission. E_{ads} and $C_{\text{site}} = \frac{4\pi R_{\text{aero}}^2}{S_{\text{site}}} C_{\text{aero}}$ are, respectively, the adsorption energy and the concentration of adsorbing sites in the air. C_{aero} and $K^0 = V_{\text{s}} e^{E_{\text{ads}}}$ are, respectively, the aerosol concentration in the air and the Langmuir chemical constant. In C_{a} and C_{g} graphs, two regions are observed, roughly separated by the $K^0 C_{\text{site}} = 1$ oblique axis. On the left side of this axis, chemical equilibrium is reached; pheromones are mainly in the gas phase, and they diffuse through gas diffusion. On the right side of the $K^0 C_{\text{site}} = 1$ axis, adsorbed pheromones dominate over gas ones. In this region, below the $t_{\text{ads}} = \frac{1}{k_{\text{ads}} C_{\text{site}}} = 100$ s horizontal axis, chemical equilibrium is not reached. The $N_{\text{a}} = \frac{C_{\text{a}}}{C_{\text{aero}}}$ graph, was computed supposing that aerosols had a radius of $0.3 \mu\text{m}$. The initial puff concentration is $C_{\text{T}}^i = 5 \times 10^9 \text{ cm}^{-3}$, and the initial puff radius is $R_{\text{i}} = 1 \text{ mm}$. Note that certain axes are log scaled.

very small (because of the low gas pheromone concentration), and N_{a} does not depend on C_{aero} either.

Aerosols are found to have as many as several thousands of pheromones on them for $E_{\text{ads}} > 30 k_{\text{B}}T$ in the situation described in Figure 5. Nevertheless, the maximal aerosol coverage that can be obtained is $C_{\text{a}}/C_{\text{site}} = 0.09 \ll 1$, confirming that saturation effects could be neglected. Finally, we demonstrated that, above a threshold for the adsorption energy, numerous pheromones are adsorbed on aerosols and maintain the pheromone concentrated for a long time; the threshold is typically for $t = 100$ s, $E_{\text{ads}} = 30 k_{\text{B}}T$, i.e., $K^0 = 10^{-10} \text{ cm}^3$.

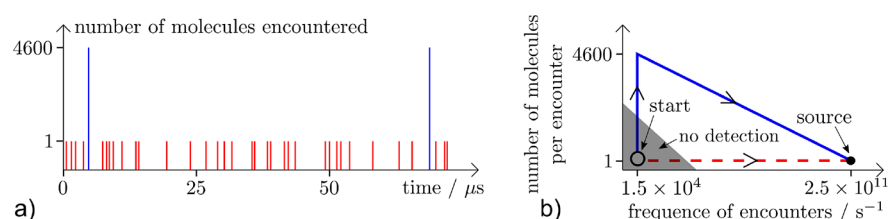


Figure 6. Illustration of antenna-pheromones encountering events for molecular and aerosol transport of pheromones (values given are only illustrative). (a) Encountering events of individual pheromones (red) and aggregated pheromones on aerosols (blue) with insect antenna. Encountering events are less frequent for aerosol transport, but many molecules arrive at the same time. (b) As the insect moves toward the source, the frequency of encountering events and number of pheromones associated evolve according to two scenarios. The red dashed curve is the scenario for pheromones following molecular transport only. The blue curve is for aerosol transport. In the shaded area, pheromones are not detected by the receptor insect because the number of molecules and the frequency of encounters are too low. In the case of aerosol transport, an insect starting far from the source (in the vertical part of the blue curve) only meets pheromones on aerosols. The number of pheromones per aerosol increases as the insect goes toward the source. In the oblique part of the blue curve, gas and adsorbed pheromones coexist as the insect is close enough to the source so that pheromones are not yet adsorbed by aerosols. Aerosol transport helps to maintain the pheromones at detectable levels.

CONSEQUENCES OF AEROSOL TRANSPORT IN CHEMICAL COMMUNICATION

A description of the aggregation dynamics of pheromones on the aerosol surface, unable to penetrate in the aerosol bulk, was achieved using the general framework introduced by Gibbs and refined by Tanford for the two-dimensional pseudophases created by amphiphilic molecules.^{4,19,26,43,44} Occupancy of the surface by aerosols can be estimated with high precision as long as the gain of energy of moving the pheromone from the gas phase to the interface can be determined. Appropriated experimental and theoretical methods can lead to such results.^{27,45–48} We developed here the generic theory in the case of independent pheromone molecules adsorbed on the surface of aerosols composed of pure water.

We showed that the energy of adsorption strongly influence (threshold effect) the proportion of pheromones adsorbed at long time. We furthermore showed that aerosol concentration modifies the adsorption kinetics of the pheromones and thus the amount of pheromones that can diffuse through gas diffusion before becoming adsorbed. Aerosol concentration determines the time, or equivalently the distance from the source, at which the adsorbed pheromones overwhelm the gas ones and at which the diffusion of the pheromone puff switches from gas to effective diffusion. However, aerosol concentration does not significantly modify the number of pheromone molecules per aerosol.

As a consequence, as long as we have some adsorbing aerosols (with $E_{\text{ads}} > 30 k_{\text{B}}T$), many pheromones can be found on each one of them. The aerosols become coated with pheromones quickly (less than 100 s) and can stay so for quite a long time in the air ($>10^3$ s), while pheromones staying in the gas phase become dispersed to undetectable concentrations rapidly due to gas diffusion. This distinction between molecular and aerosol transport mechanisms has great consequences in the way we picture the transport of pheromones. The spatial distribution of pheromones following molecular transport would be widespread, as a puff becomes larger and larger and less and less dense. By contrast, pheromones following aerosol transport would be distributed as dense spots, and hence strong olfactory clues, that last for a long time. As a consequence, many molecules, on a single aerosol, arriving on an insect at the same time might trigger an olfactory detection (Figure 6).

The number of molecules that can accumulate on the surface of one aerosol depends on relative humidity as it increases aerosol water content and size.¹⁵ More generally, humidity has been observed to influence moth pheromonal communication.⁴⁹ Our general theory might offer the first clues to understand the mechanisms underlying these observations. Progress in this direction depends on experimental advances in order to characterize the molecules transported in one aerosol of control type and history.^{17,47} Proper characterization of aerosol surface composition and properties is still a challenging task and is limited to rare studies.^{17,18} Further investigation would need to discriminate which values of parameters are mostly fitting a specific chemical communication context.

More complex effects, beyond the description of adsorption of individual molecules at the pure water surface, might come into play in the aerosol transport of pheromones. Interactions with all surface-active species (i.e., organic and hydrophobic molecules, surfactants, hydrotropes, salts^{19,50–53}) and especially nanoparticles⁵⁴ affect the content of the surface. Adsorbed species can either favor the adsorption of pheromones via a cosurfactant effect or hinder it due to crowding. Thus, strong antagonistic as well as synergistic effects are expected.^{19,51,53} Other biogenic surfactants in the air can compete with pheromones for adsorption on aerosols and saturate the surface. Saturation of aerosols includes nonlinear effects in pheromone transport and hampers aerosol transport (see Appendix B). Inhibition of the pheromonal response in given insects in the presence of specific plant volatiles has been reported.⁵⁵ Saturation of aerosols by the plant volatiles⁴⁷ or other physicochemical effects might reduce pheromone detection by the insects. Saturation of aerosols can also occur by smaller poorly labile aerosols, such as airborne solid carbon residues of combustion that are one major issue in large cities.¹⁴ The number of small aerosols needed to saturate the surface of a bigger one is $4f^2$ where f is the ratio between the radius of the bigger and small aerosols. For $f = 10$, it gives 400 small aerosols for every bigger one, a ratio which holds within polluted air records.^{14,15} Moreover, adsorption on aerosol can increase pheromone degradation speed by collecting pheromones and reactive species together at the surface.^{17,46,56,57} On the other hand, mixtures of surface-active molecules can be chosen with a specific blend so that their adsorption properties are enhanced.^{19,53} Pheromones are known to often be released with accurate blend ratios,^{3,12} but there is no current

explanation on how these blends could remain stable from emitter gland to receptor insect. Aggregation and synergistic effects might occur between the molecules of the blend and help to maintain a stable ratio between the molecules. Synergies can also occur with other molecules released by plants in the insect habitat.^{47,55,56} Some effects favoring or hampering aerosol transport might be applied for the design of sustainable methods in pest control using volatile dispensers or multicropping systems.^{56,58} In the model we developed, the concentration of adsorption sites is the same everywhere in the air, and the adsorption energy does not vary from one site to another. In practice, these quantities inherently fluctuate. See the [Supporting Information](#), section D, for further discussion on how our model relates to such a context.

Finally, we propose that certain molecules synthesized by insects for communicating evolved into molecules adapted to adsorb on the aerosols naturally present in the air. The concerned molecules use a communication path different from molecules staying in the gas phase and increase persistence of the signal in the air. Moreover, capture of aerosols by insect antennae differ from capture of individual molecules. Interaction between insect olfactory organs (sensilla) and aerosols might be governed by wetting and coalescing dynamics as well as colloidal and electrostatic interactions,^{26,59} enhancing the capture by increasing the cross-section area of the sensor.^{60,61} Accurate modeling of the pheromone path from release to reception in a way that explains observed performances of insect mate finding⁶² has not been reached yet. Pheromone uptake by aerosol has not been considered so far. We showed here that aerosol transport maintains olfactory clues over long distances (see [Figure 6](#)) and is a new efficient channel for communication. The approach used here, inherited from the field of physicochemistry, was a key element to formulate this problem. A further understanding of interactions between olfactory molecules in the atmosphere in the frame of physicochemistry can have direct applications, in particular in the improvement of insect pest control, as well as fundamental consequences in the understanding of ecological interactions.^{3,63–66}

■ APPENDIX A: COMPUTING THE ADSORPTION REACTION CONSTANT

We consider surfactant molecules moving between the air and water interface. We aim to compute $V(z)$, the free energy of a molecule at position z from the interface, averaged over all the solvent configurations and molecule orientations (which corresponds to the McMillan–Mayer potential⁶⁷). Following Ivanov and collaborators' works,^{24,25} we suppose that $V(z) = 0$ in the air for $z < 0$ and in the water for $z > 0$:

$$V(z) = -V_0 + \frac{\Delta\mu_{\text{CH}_2}}{l_{\text{CH}_2}}z \quad (\text{A1})$$

V_0 is the free energy gain when moving the molecule from gas to the interface. $\frac{\Delta\mu_{\text{CH}_2}}{l_{\text{CH}_2}}$ is the energy cost per unit of length when the molecule penetrates in the water phase as the carbon chain becomes hydrated. An illustration of this formula is given in [Figure A1](#). V_0 has several contributions:

$$V_0 = E_{\text{head}} + \gamma S_{\text{site}} - F_{\text{rot}} = E_{\text{ads}} - F_{\text{rot}} \quad (\text{A2})$$

$F_{\text{rot}} = k_{\text{B}}T \ln 2$ is the free energy (entropic) cost due to the fact that the molecule at the interface is constrained to rotate only

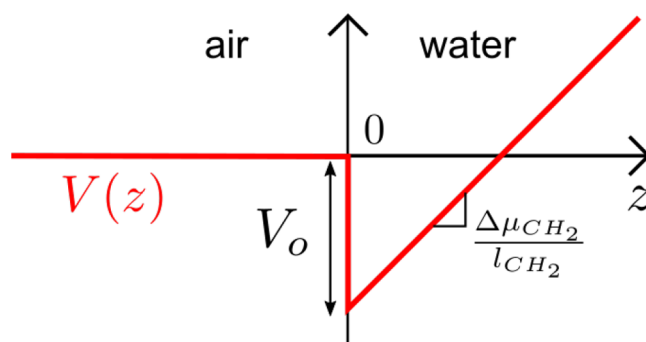


Figure A1. Free energy profile of the nonsoluble surfactant at the water–air interface, following Ivanov and collaborators.^{24,25}

in a half space. E_{head} and γS_{site} contributions were already specified in the main text. Distribution of surfactant molecules is then given by $C(z) = C_{\text{g}} \exp\left(-\frac{V(z)}{k_{\text{B}}T}\right)$, and the surface density of surfactants reads $\Gamma_{\text{a}} = \int_0^{\infty} C(z) dz$. We thus find

$$\Gamma_{\text{a}} = C_{\text{g}} \delta e^{E_{\text{ads}}/k_{\text{B}}T} \quad (\text{A3})$$

The Langmuir equilibrium for low molecule density reads $K^0 = \frac{C_{\text{a}}}{C_{\text{site}} C_{\text{g}}}$. The concentration of adsorbed pheromones and adsorption sites further reads $C_{\text{a}} = C_{\text{aero}} \frac{4}{3} \pi R_{\text{aero}}^2 \Gamma_{\text{a}}$ and $C_{\text{site}} = C_{\text{aero}} \frac{4}{3} \frac{\pi R_{\text{aero}}^2}{S_{\text{site}}}$ so that their ratio is $\frac{C_{\text{a}}}{C_{\text{site}}} = \Gamma_{\text{a}} S_{\text{site}}$. Finally, we find $K^0 = S_{\text{site}} \delta e^{E_{\text{ads}}/k_{\text{B}}T}$ as given in [eq 3](#).

■ APPENDIX B: DYNAMICS OF PHEROMONE TRANSPORT WHEN AEROSOLS CAN SATURATE

Dynamics of pheromone transport in the case of saturating aerosols can be described within the frame of fast variable elimination.⁶⁸ The reaction-diffusion [eqs 13](#) and [14](#) are solved within the limit of fast chemistry: $k_{\text{abs}} \rightarrow +\infty$. C_{a} and C_{g} are fast variables because $\frac{\partial C_{\text{a}}}{\partial t}$ and $\frac{\partial C_{\text{g}}}{\partial t} \rightarrow +\infty$ within this limit. On the other hand the total pheromone concentration $C_{\text{T}} = C_{\text{a}} + C_{\text{g}}$ follows

$$\frac{\partial C_{\text{T}}}{\partial t} = \nabla \cdot (D_{\text{g}} \nabla C_{\text{g}} + D_{\text{a}} \nabla C_{\text{a}}) \quad (\text{A4})$$

and $\frac{\partial C_{\text{T}}}{\partial t}$ does not diverge when $k_{\text{abs}} \rightarrow +\infty$. C_{T} can be considered as a slow variable for which the evolution is much slower than the one of C_{a} and C_{g} . Instantaneously, the fast variables C_{a} and C_{g} react, and they follow the variation of the slow variable C_{T} . This *slavery* of C_{a} and C_{g} is valid if one considers time scales longer than the chemical scale $t \gg t_{\text{c}}$. In that case, the distribution ratio of gas and adsorbed pheromones adapt locally to equilibrium value on a time scale way shorter than the one with which C_{T} evolves. It is thus fixed by [eq 1](#) and the local value of C_{T} . We replace C_{g} and C_{a} by $C_{\text{g}}(C_{\text{T}})$ and $C_{\text{a}}(C_{\text{T}})$ in [eq A4](#) to find

$$\frac{\partial C_{\text{T}}}{\partial t} = \nabla \cdot (D_{\text{eff}}(C_{\text{T}}) \nabla C_{\text{T}}) \quad (\text{A5})$$

with

$$D_{\text{eff}}(C_T) = D_g \frac{dC_g}{dC_T} + D_a \frac{dC_a}{dC_T} \quad (\text{A6})$$

These general formulas mean that the pheromone transport follows a space-dependent Fick's law for which the local diffusion coefficient is D_{eff} . For nonsaturating aerosols, equilibrium reduces to $\frac{C_g}{C_a} = K^0 C_s$, and we recover the result given in eq 23. The effective diffusion coefficient of the pheromone is an average of the one of the gas and the aerosol. On the other hand, for saturated aerosols, $C_a = C_s$ and $C_g = C_T - C_s$ so that $D_{\text{eff}} = D_g$. The saturation of the aerosols prevents them from retaining the pheromones. At any time, as soon as the aerosols are saturated, they can no longer store the molecules which then diffuse with the gas diffusion coefficient. The containment of pheromones during transport by means of aerosols can therefore only take place as long as the aerosols are not saturated.

■ ASSOCIATED CONTENT

Supporting Information

The Supporting Information is available free of charge at <https://pubs.acs.org/doi/10.1021/acscentsci.0c00892>.

Results when adsorption kinetics is limited, further justifications of the applicability of a linear model, data showing the negligible influence of the varying aerosol diffusion coefficient, and a discussion on how our model relates to a realistic fluctuating environment (PDF)

■ AUTHOR INFORMATION

Corresponding Author

Jean-François Dufreche – ICSM, CEA, CNRS, ENSCM, Univ Montpellier, 30207 Bagnols-sur-Cèze, France; orcid.org/0000-0001-8422-3639; Email: jean-francois.dufreche@umontpellier.fr

Authors

Ludovic Jami – ICSM, CEA, CNRS, ENSCM, Univ Montpellier, 30207 Bagnols-sur-Cèze, France; orcid.org/0000-0002-8822-7669

Thomas Zemb – ICSM, CEA, CNRS, ENSCM, Univ Montpellier, 30207 Bagnols-sur-Cèze, France; orcid.org/0000-0001-8410-6969

Jérôme Casas – Institut de Recherche sur la Biologie de l'Insecte, UMR 7261, CNRS—Université de Tours, 37200 Tours, France; orcid.org/0000-0003-1666-295X

Complete contact information is available at:

<https://pubs.acs.org/doi/10.1021/acscentsci.0c00892>

Author Contributions

All the authors planned together this research work. L.J. and J.-F.D. conducted the modeling. J.C. and T.Z. provided data and analysis from, respectively, insect ecology and microphases' physicochemistry. L.J. wrote the manuscript, and all authors contributed to its editing.

Notes

The authors declare no competing financial interest.

■ ACKNOWLEDGMENTS

We thank Claudio Lazzari, Christophe Bressac, Lolita Hilaire, and Bertrand Siboulet for fruitful discussions. The work was supported by the Project PHEROAERO from the Region

Centre and by a ENS Lyon Ph.D. fellowship to L.J. in Tours under the supervision of J.C. and J.-F.D.

■ REFERENCES

- (1) Bossert, W. H.; Wilson, E. O. The analysis of olfactory communication among animals. *J. Theor. Biol.* **1963**, *5*, 443–469.
- (2) Murlis, J.; Elkinton, J. S.; Carde, R. T. Odor plumes and how insects use them. *Annu. Rev. Entomol.* **1992**, *37*, 505–532.
- (3) Pannunzi, M.; Nowotny, T. Odor stimuli: Not just chemical identity. *Front. Physiol.* **2019**, *10*, 1428.
- (4) Kronberg, B.; Holmberg, K.; Lindman, B. *Surface chemistry of surfactants and polymers*; John Wiley & Sons, 2014.
- (5) Kunz, W.; Holmberg, K.; Zemb, T. Hydrotropes. *Curr. Opin. Colloid Interface Sci.* **2016**, *22*, 99–107.
- (6) Schöttl, S.; Horinek, D. Aggregation in detergent-free ternary mixtures with microemulsion-like properties. *Curr. Opin. Colloid Interface Sci.* **2016**, *22*, 8–13.
- (7) Regnier, F. E.; Law, J. H. Insect pheromones. *J. Lipid Res.* **1968**, *9*, 541–551.
- (8) *chemspider*. <http://www.chemspider.com> (accessed 2020-04-09).
- (9) Ando, T.; Inomata, S.-i.; Yamamoto, M. *The chemistry of pheromones and other Semiochemicals I*; Springer, 2004; pp 51–96.
- (10) Krasnoff, S. B.; Roelofs, W. L. Sex pheromone released as an aerosol by the moth *Pyrrharctia isabella*. *Nature* **1988**, *333*, 263–265.
- (11) Kuba, H.; Sokei, Y. The production of pheromone clouds by spraying in the melon fly, *Dacus cucurbitae* Coquillett (Diptera: Tephritidae). *Journal of Ethology* **1988**, *6*, 105–110.
- (12) Schal, C.; Charlton, R. E.; Cardé, R. T. Temporal patterns of sex pheromone titers and release rates in *Holomelina lamae* (Lepidoptera: Arctiidae). *J. Chem. Ecol.* **1987**, *13*, 1115–1129.
- (13) Jaenicke, R. Natural aerosols. *Ann. N. Y. Acad. Sci.* **1980**, *338*, 317–329.
- (14) Jaenicke, R. *International Geophysics*; Elsevier, 1993; Vol. 54, pp 1–31.
- (15) Friedlander, S. K.; et al. *Smoke, dust, and haze*; Oxford University Press: New York, 2000; Vol. 198.
- (16) Carslaw, K.; Boucher, O.; Spracklen, D.; Mann, G.; Rae, J.; Woodward, S.; Kulmala, M. A review of natural aerosol interactions and feedbacks within the Earth system. *Atmos. Chem. Phys.* **2010**, *10*, 1701.
- (17) Donaldson, D.; Vaida, V. The influence of organic films at the air–aqueous boundary on atmospheric processes. *Chem. Rev.* **2006**, *106*, 1445–1461.
- (18) Tervahattu, H.; Juhanoja, J.; Vaida, V.; Tuck, A.; Niemi, J. V.; Kupiainen, K.; Kulmala, M.; Vehkamäki, H. Fatty acids on continental sulfate aerosol particles. *J. Geophys. Res.* **2005**, *110*, D06207.
- (19) Li, S.; Cheng, S.; Du, L.; Wang, W. Establishing a model organic film of low volatile compound mixture on aqueous aerosol surface. *Atmos. Environ.* **2019**, *200*, 15–23.
- (20) Claeys, M.; Graham, B.; Vas, G.; Wang, W.; Vermeylen, R.; Pashynska, V.; Cafmeyer, J.; Guyon, P.; Andreae, M. O.; Artaxo, P.; et al. Formation of secondary organic aerosols through photo-oxidation of isoprene. *Science* **2004**, *303*, 1173–1176.
- (21) Rizzo, L.; Artaxo, P.; Karl, T.; Guenther, A.; Greenberg, J. Aerosol properties, in-canopy gradients, turbulent fluxes and VOC concentrations at a pristine forest site in Amazonia. *Atmos. Environ.* **2010**, *44*, 503–511.
- (22) Pöhlker, C.; Wiedemann, K. T.; Sinha, B.; Shiraiwa, M.; Gunthe, S. S.; Smith, M.; Su, H.; Artaxo, P.; Chen, Q.; Cheng, Y.; et al. Biogenic potassium salt particles as seeds for secondary organic aerosol in the Amazon. *Science* **2012**, *337*, 1075–1078.
- (23) Zhu, C.; Kawamura, K.; Fukuda, Y.; Mochida, M.; Iwamoto, Y. Fungal spores overwhelm biogenic organic aerosols in a midlatitudinal forest. *Atmos. Chem. Phys.* **2016**, *16*, 7497–7506.
- (24) Slavchov, R. I.; Ivanov, I. B. Effective osmotic cohesion due to the solvent molecules in a delocalized adsorbed monolayer. *J. Colloid Interface Sci.* **2018**, *532*, 746–757.

- (25) Slavchov, R. I.; Ivanov, I. B. Adsorption parameters and phase behaviour of non-ionic surfactants at liquid interfaces. *Soft Matter* **2017**, *13*, 8829–8848.
- (26) Israelachvili, J. N. *Intermolecular and surface forces*; Academic press, 2015.
- (27) Liyana-Arachchi, T. P.; Zhang, Z.; Vempati, H.; Hansel, A. K.; Stevens, C.; Pham, A. T.; Ehrenhauser, F. S.; Valsaraj, K. T.; Hung, F. R. Green leaf volatiles on atmospheric air/water interfaces: A combined experimental and molecular simulation study. *J. Chem. Eng. Data* **2014**, *59*, 3025–3035.
- (28) Marek, R.; Straub, J. Analysis of the evaporation coefficient and the condensation coefficient of water. *Int. J. Heat Mass Transfer* **2001**, *44*, 39–53.
- (29) Tsuruta, T.; Nagayama, G. A microscopic formulation of condensation coefficient and interface transport phenomena. *Energy* **2005**, *30*, 795–805.
- (30) Nagayama, G.; Takematsu, M.; Mizuguchi, H.; Tsuruta, T. Molecular dynamics study on condensation/evaporation coefficients of chain molecules at liquid–vapor interface. *J. Chem. Phys.* **2015**, *143*, No. 014706.
- (31) Persad, A. H.; Ward, C. A. Expressions for the evaporation and condensation coefficients in the Hertz-Knudsen relation. *Chem. Rev.* **2016**, *116*, 7727–7767.
- (32) Varilly, P.; Chandler, D. Water evaporation: A transition path sampling study. *J. Phys. Chem. B* **2013**, *117*, 1419–1428.
- (33) Julin, J.; Shiraiwa, M.; Miles, R. E.; Reid, J. P.; Pöschl, U.; Riipinen, I. Mass accommodation of water: Bridging the gap between molecular dynamics simulations and kinetic condensation models. *J. Phys. Chem. A* **2013**, *117*, 410–420.
- (34) Julin, J.; Winkler, P. M.; Donahue, N. M.; Wagner, P. E.; Riipinen, I. Near-unity mass accommodation coefficient of organic molecules of varying structure. *Environ. Sci. Technol.* **2014**, *48*, 12083–12089.
- (35) Bley, M.; Duvail, M.; Guilbaud, P.; Dufrière, J.-F. Simulating Osmotic Equilibria: A New Tool for Calculating Activity Coefficients in Concentrated Aqueous Salt Solutions. *J. Phys. Chem. B* **2017**, *121*, 9647–9658.
- (36) Zwanzig, R. *Nonequilibrium Statistical Mechanics*; Oxford University Press, 2001.
- (37) Pöschl, U.; Rudich, Y.; Ammann, M. Kinetic model framework for aerosol and cloud surface chemistry and gas-particle interactions ? Part 1: General equations, parameters, and terminology. *Atmos. Chem. Phys.* **2007**, *7*, 5989–6023.
- (38) Umbers, K. D. L.; Symonds, M. R. E.; Kokko, H. The Mathematics of Female Pheromone Signaling: Strategies for Aging Virgins. *Am. Nat.* **2015**, *185*, 417–432.
- (39) Foster, S. P.; Anderson, K. G.; Casas, J. The dynamics of pheromone gland synthesis and release: a paradigm shift for understanding sex pheromone quantity in female moths. *J. Chem. Ecol.* **2018**, *44*, 525–533.
- (40) Bird, R. B.; Stewart, W. E. *Transport phenomena*, 2nd ed.; John Wiley & Sons, 2007; Chapter 19, pp 582–606.
- (41) Turq, P.; Barthel, J.; Chemla, M. *Transport, Relaxation and Kinetic Processes in Electrolyte Solutions*; Springer-Verlag, 1992.
- (42) Berne, B. J.; Pecora, R. *Dynamic Light Scattering*; Dover, 2000.
- (43) Tanford, C. Hydrophobic free energy, micelle formation and the association of proteins with amphiphiles. *J. Mol. Biol.* **1972**, *67*, 59–74.
- (44) Tanford, C. *The hydrophobic effect: formation of micelles and biological membranes*, 2nd ed.; J. Wiley, 1980.
- (45) Massoudi, R.; King, A., Jr Effect of pressure on the surface tension of water. Adsorption of low molecular weight gases on water at 25. deg. *J. Phys. Chem.* **1974**, *78*, 2262–2266.
- (46) Valsaraj, K. T. A review of the aqueous aerosol surface chemistry in the atmospheric context. *Open J. Phys. Chem.* **2012**, *2* (1), 58.
- (47) Ren, Y.; McGillen, M.; Daële, V.; Casas, J.; Mellouki, W. The fate of methyl salicylate in the environment and its role as signal in multitrophic interactions. *Sci. Total Environ.* **2020**, 141406.
- (48) De Angelis, P.; Cardellini, A.; Asinari, P. Exploring the Free Energy Landscape To Predict the Surfactant Adsorption Isotherm at the Nanoparticle–Water Interface. *ACS Cent. Sci.* **2019**, *5*, 1804–1812.
- (49) McNeil, J. N. Behavioral ecology of pheromone-mediated communication in moths and its importance in the use of pheromone traps. *Annu. Rev. Entomol.* **1991**, *36*, 407–430.
- (50) Kunz, W. *Specific ion effects*; World Scientific, 2010.
- (51) Demou, E.; Donaldson, D. Adsorption of atmospheric gases at the air–water interface. 4: The influence of salts. *J. Phys. Chem. A* **2002**, *106*, 982–987.
- (52) Brzozowska, A.; Duits, M. H.; Mugele, F. Stability of stearic acid monolayers on Artificial Sea Water. *Colloids Surf., A* **2012**, *407*, 38–48.
- (53) Špadina, M.; Bohinc, K.; Zemb, T.; Dufrière, J.-F. Synergistic Solvent Extraction Is Driven by Entropy. *ACS Nano* **2019**, *13*, 13745–13758.
- (54) Binks, B. P.; Yin, D. Pickering emulsions stabilized by hydrophilic nanoparticles: in situ surface modification by oil. *Soft Matter* **2016**, *12*, 6858–6867.
- (55) Reddy, G. V.; Guerrero, A. Interactions of insect pheromones and plant semiochemicals. *Trends Plant Sci.* **2004**, *9*, 253–261.
- (56) Conchou, L.; Lucas, P.; Meslin, C.; Proffit, M.; Staudt, M.; Renou, M. Insect odorscapes: from plant volatiles to natural olfactory scenes. *Front. Physiol.* **2019**, *10*, 972.
- (57) Donaldson, D.; Valsaraj, K. T. Adsorption and reaction of trace gas-phase organic compounds on atmospheric water film surfaces: A critical review. *Environ. Sci. Technol.* **2010**, *44*, 865–873.
- (58) Mofikoya, A. O.; Bui, T. N. T.; Kivimäenpää, M.; Holopainen, J. K.; Himanen, S. J.; Blande, J. D. Foliar behaviour of biogenic semi-volatiles: potential applications in sustainable pest management. *Arthropod-Plant Interactions* **2019**, *13*, 193–212.
- (59) Carroll, B. The accurate measurement of contact angle, phase contact areas, drop volume, and Laplace excess pressure in drop-on-fiber systems. *J. Colloid Interface Sci.* **1976**, *57*, 488–495.
- (60) Jaffar-Bandjee, M.; Steinmann, T.; Krijnen, K.; Casas, J. Leakiness and flow capture rate ratio of insect pectinate antenna. *J. R. Soc., Interface* **2020**, *17*, 20190779.
- (61) Spencer, T. L.; Mohebbi, N.; Jin, G.; Forister, M. L.; Alexeev, A.; Hu, D. L. Moth-inspired methods for particle capture on a cylinder. *J. Fluid Mech.* **2020**, *884*, 927.
- (62) Wall, C.; Perry, J. Range of action of moth sex-attractant sources. *Entomol. Exp. Appl.* **1987**, *44*, 5–14.
- (63) Koehl, M. Physical modelling in biomechanics. *Philos. Trans. R. Soc., B* **2003**, *358*, 1589–1596.
- (64) Denny, M. *Ecological mechanics: Principles of life's physical interactions*; Princeton University Press, 2015.
- (65) Yohe, L. R.; Brand, P. Evolutionary ecology of chemosensation and its role in sensory drive. *Curr. Zool.* **2018**, *64*, 525–533.
- (66) Katsnelson, A. Decoding an Insects Sensory World. *ACS Cent. Sci.* **2018**, *4*, 785.
- (67) McMillan, W. G., Jr; Mayer, J. E. The statistical thermodynamics of multicomponent systems. *J. Chem. Phys.* **1945**, *13*, 276–305.
- (68) Van Kampen, N. G. Elimination of fast variables. *Phys. Rep.* **1985**, *124*, 69–160.